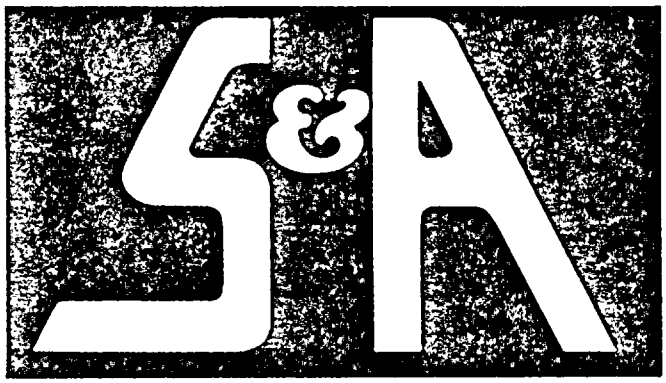

SEISMIC QUALIFICATION REPORT FOR

THE REFUELING WATER STORAGE TANK

AT THE R. E. GINNA PLANT

STEVENSON & ASSOCIATES

a structural-mechanical consulting engineering firm

9217 Midwest Avenue
Cleveland, Ohio 44125
(216) 587-3805
TELEX: 985570

458 Boston St., Suite #3
Topsfield, MA 01983
(617) 887-5688

SEISMIC QUALIFICATION REPORT FOR THE REFUELING WATER STORAGE TANK AT THE R. E. GINNA PLANT

Prepared for

ROCHESTER GAS & ELECTRIC COMPANY
89 East Avenue
Rochester, New York

August 1983

Prepared by

STEVENSON & ASSOCIATES
458 Boston Street
Topsfield, Massachusetts

CERTIFICATION

The undersigned, a registered Professional Engineer, competent in the field of component stress analysis, certifies that to the best of his knowledge and belief the analysis calculations for the subject tank as presented in this seismic stress report comply with the provisions of the applicable portions of the ASME Boiler and Pressure Vessel Code, Section III, Nuclear Power Plant Components and standard acceptable engineering practice.

Component: Refueling Water Storage Tank
Plant: R. E. Ginna

John D. Stevenson

Dr. John D. Stevenson

5&A

SEISMIC QUALIFICATION REPORT FOR
THE REFUELING WATER STORAGE TANK
AT THE R. E. GINNA PLANT
Revision 0, August 1983

Prepared by _____
Dr. Tsi-Ming Tseng

Reviewed by _____
Stephen Anagnostis, Project Manager

Reviewed by _____
Dr. Jerome J. Connor

Approved by _____
Dr. John D. Stevenson

TABLE OF CONTENTS

FIGURES

FIGURES (Continued)

TABLES

1. INTRODUCTION

The ability of the refueling water storage tank (RWST) to withstand dead weight and seismic forces is investigated in this evaluation.

The RWST is a thin, cylindrical shell with a flat circular bottom and a fixed dome roof. The design temperature is 200^{0}F. The RWST is classified as an ASME Class 2 atmospheric storage tank. Anchorage consists of thirty (30) cast-in-place bolts equally spaced around the tank bottom. The analysis assumes the RWST is filled with water to its maximum capacity (331,000 gallons). Lower fill levels were investigated -- the maximum fill level proved to be the worst case.

Analysis loads consist of the dead weight of the tank and contents, and seismic loads in two horizontal and the vertical directions. The seismic loads are defined by the site specific ground response spectrum for R. E. Ginna as specified by the USNRC [23]. The full spectrum is used for the horizontal analysis. Two thirds of the full spectrum is used for the vertical analysis.

The dynamic response analysis follows the requirements of NUREG/CR-1161 [16]. Analysis of the convective (sloshing) horizontal response is performed using the conventional "rigid tank" assumptions as outlined by Haroun [7]. Tank flexibility and fluid-structure interaction is incorporated in the analysis of the impulsive (non-sloshing) horizontal response. The impulsive analysis is performed using an extension of the approximate method developed by Fujita and Shiraki [5]. Tank flexibility is also incorporated in the vertical response analysis per the development by Rigaudeau [18]. A damping level of 1/2% is used for the convective horizontal response analysis (Reference 16, p. 29). Consistent with the discussion in NUREG/CR-1821 [17], 7% damping is used for the impulsive horizontal and vertical response analyses.

The acceptance criteria consider the following principle points:

1. Anchorage Stresses: These include the stresses in the bolts, brackets, and bracket welds. Allowables are calculated per Reference 1, Subarticle NF 3300.

2. Tank Wall Material Stress: The axial, hoop, and shear stresses developed in the tank wall are compared to material allowables per Reference 1, Subarticle NC 3800.

3. Tank Wall Buckling: The axial, hoop, and shear stresses developed in the tank wall are compared to experimentally derived buckling criteria [3, 4, 6, 8-15, 19-22, 25, 26].

The results of the analysis are summarized in Tables 3 and 4. The evaluation shows that the RWST is adequately designed to withstand dead weight loads in combination with the postulated seismic event.

2. DESCRIPTION OF THE RWST

The RWST is a thin, cylindrical shell welded to a flat circular bottom and a spherical roof (Figure 1). The cylindrical shell is 26'-6" in diameter and 81'-0" high. The shell is 5/16" thick for the first 8'-1/8", 9/32" thick for the next 8'-1-1/8", and 1/4" thick for the remainder of the height. The bottom plate is 26'-10" in diameter and 1/4" thick. The spherical roof has a radius of 26'-0" and a thickness of 3/16". All tank material is Type 304 stainless steel.

In this evaluation, stresses are calculated at three elevations in the tank shell (Elevations 16'-2-1/4", 8'-1-1/8", and 0'-0" in Figure 1). These are the levels of maximum stress for the three different tank thicknesses (1/4", 9/32", and 5/16").

The anchorage consists of thirty (30), 2-1/4" diameter, A36 Bolts, equally spaced around the tank diameter (Figure 2). The bolts are attached to the tank wall via the bracket shown in Figures 2 and 3. Note that the brackets have been modified since the original installation of the tank. All bracket material is assumed to be A36 steel. All bracket welds are assumed to be E308 and E309 electrodes.

The tank is assumed filled to its maximum water level -- 6" below the top of the cylindrical shell. This corresponds to a water volume of 331,000 gallons. The total weight of the RWST is 2,850 kips -- 2,773 kips of water and 77 kips of steel.

3. SEISMIC CRITERIA

The site specific ground response spectrum for R. E. Ginna, as specified by the USNRC [23], is used in this analysis. Figure 4 shows the spectrum for a damping level of 7%. The full spectrum is used for the horizontal response analysis. Two thirds of the full spectrum is used for the vertical response analysis.

Per the recommendation of Reference 16, 0.5% damping is used for the analysis of the horizontal convective mode.

Damping values used in NUREG/CR-1821 [17] for the impulsive response analysis of tanks vary between 4% and 7%. The lower value of 4% governs when the expected lower bound mode of failure is controlled by stresses in the tank wall (welded construction). The high damping value of 7% governs when the expected lower bound failure mode is controlled by yield or tensile deformation of anchor bolts. From Tables 3 and 4 it can be seen that the safety factor calculated for tensile failure of the anchor bolts is 1.30, while the lowest safety factor in the steel shell is 1.56. Hence bolting and 7% damping governs the analysis.

Due to the axisymmetric geometry of the RWST, only one horizontal seismic response analysis is required to evaluate the effect of two perpendicular horizontal earthquakes. As is discussed in Section 4, the horizontal response can be described by axial, hoop, and shear stresses in the tank wall, and tensile forces on the bolt/bracket anchorages. For a single horizontal earthquake, the maximum tank wall normal (hoop and axial) stresses and the maximum tank wall shear stresses occur 90^{o} apart on the tank circumference. The distribution of these stresses around the tank circumference is such that an SRSS, at any point around the circumference, of co-directional stresses resulting from two perpendicular horizontal earthquakes would result in a stress field at that point consisting of the maximum normal stresses and maximum shear stress found from the single earthquake analysis. Thus the effect of two horizontal earthquakes is accounted for by performing a response analysis for a single earthquake and then evaluating the resulting stresses under the assumption that the maximum tank wall normal stresses and maximum tank wall shear stresses occur at the same point.

Similarly, the distribution of anchorage forces around the tank circumference is such that an SRSS of anchor forces, at any point, due to perpendicular, horizontal earthquakes is equal to the maximum anchor force calculated due to a single earthquake. Thus only a single horizontal resultant response analysis is required.

4 ANALYSIS PROCEDURE

4.1 Dead Load

The dead load of the steel results in axial stresses in the tank shell:

$$\sigma_\phi(x) = W(x)/2\pi Rh(x) \qquad (4.1)$$

The dead load of the water results in hoop stresses in the tank shell:

$$\sigma_\theta(x) = \rho g(H-x)R/h(x) \qquad (4.2)$$

The dead load stresses are tabulated in Table 2.

4.2 Horizontal Seismic

4.2.1 Convective Response

Per Reference 7, the sloshing frequency, weight, and elevation are calculated as follows:

$$f_s = \frac{1}{2\pi}\left(\frac{1.84g}{R}\tanh\left(\frac{1.84H}{R}\right)\right)^{1/2} = 0.34 \text{ Hz} \qquad (4.3)$$

$$W_s = 0.455\pi\rho g R^3 \tanh\left(\frac{1.84H}{R}\right) = 207 \text{ kips} \qquad (4.4)$$

$$H_s = H\left(1-\left(\frac{R}{1.84H}\tanh\left(\frac{.92H}{R}\right)\right)\right) = 879 \text{ in.} \qquad (4.5)$$

To complete the convective mode analysis, the spectral acceleration at 0.34 Hz and 0.5% damping is required. The response spectrum (Figure 4) is not defined below 1 Hz, nor is the procedure provided by the USNRC in

Reference 1 for adjusting the spectrum as a function of damping strictly valid for damping values less than 2%. However, the spectrum and the damping adjustment procedure were conservatively extrapolated to yield a spectral acceleration of 0.097g.

With the above results, the moment and shear at any elevation in the tank can be calculated. Those loads result in the stresses listed in Table 1.

The maximum slosh height, which occurs at a radius of 13'-3", is calculated as follows [16]:

$$d_s = 0.84(0.097g)R = 12.8 \text{ in.} \qquad (4.6)$$

The freeboard at the point of maximum slosh height is 6". Since the slosh height exceeds the freeboard, the mass of sloshing liquid will impact the tank roof. However, as the slosh height exceeds the freeboard by one 6.8" at the outer radius (13'=3") of the tank, and as the freeboard -- due to the tank roof's spherical shape -- increases rapidly with decreasing radius (the freeboard at a radius of 12'-3" is 12.8"), no significant pressure on the tank roof is expected to develop. In the worst case, rupture of the joint between the tank's roof and cylindrical shell would result in a small amount of leakage (less than 0.7% of the total volume) from the top of the tank, but the tank's structural integrity is maintained.

4.2.2 Impulsive Response

Rigorous analysis of the impulsive response requires consideration of the interaction of the fluid mass and the flexible tank walls. Haroun [7] developed a boundary element/finite element model of the fluid/structure system. Haroun presents tabulated results for the response of the fundamental impulsive mode. These results are limited to tanks of uniform thickness and a height to radius ratio (H/R) less than 3.4. The RWST, with an H/R of 6.1 and a nonconstant thickness, falls outside the range of Haroun's tabulated results. Haroun's results are, however, used to verify the approximate analysis method developed below.

Fujita [5] presents an approximate method for incorporating the fluid/structure interaction in a beam analysis of the tank. For a pure bending beam, the equation of motion is written:

$$EI\frac{\partial^4 w(x,t)}{\partial x^4} + \left(m(x) + \frac{p(x,t)}{g}\right)\frac{\partial^2 w(x,t)}{\partial t^2} = -\left(m(x) + \frac{p(x,t)}{g}\right)\frac{\partial^2 z(t)}{\partial t^2} \tag{4.7}$$

The force per unit length due to the fluid pressure, which is found by solving Laplace's equation for the fluid, can be written:

$$p(x,t) = \rho g \pi R \sum_{i=o}^{\infty} \left(\frac{2I_1(\lambda_i R)}{\lambda_i I_1'(\lambda_i R)} \cos(\lambda_i x) \int_0^H \ddot{w}(x,t)\cos(\lambda_i x)dx\right) \tag{4.8}$$

Fujita suggests solving Equation (4.6) by assuming the normal modes of the fluid/structure system to be the same as those of the tank analyzed as a beam with the fluid modeled as dead mass (i.e., the fluid pressure is equal to the fluid mass times the tank wall acceleration). This assumption allows the modal frequencies, modal participation factors, and the modal force per unit length due to fluid pressure of the fluid/structure system to be written as follows:

$$\omega_i = \left[\frac{\int_0^H (m(x)+\pi R^2 \rho)\tilde{\phi}_i^2(x)dx}{\int_0^H (m(x) + \frac{1}{g} p_i(x))\tilde{\phi}_i^2(x)dx}\right]^{\frac{1}{2}} \tilde{\omega}_i \tag{4.9a}$$

$$\Gamma_i = \frac{\int_0^H (m(x) + \frac{1}{g} p_i(x))\tilde{\phi}_i(x)dx}{\int_0^H (m(x) + \frac{1}{g} p_i(x))\tilde{\phi}_i^2(x)dx} \tag{4.9b}$$

$$p_i(x) = \rho g \pi R \sum_{i=o}^{\infty} \left(\frac{2I_1(\lambda_i R)}{\lambda_i I_1'(\lambda_i R)} \cos(\lambda_i x) \int_0^H \tilde{\phi}_i(x)\cos(\lambda_i x)dx\right) \tag{4.9c}$$

The response of the system can then be calculated using standard response spectrum techniques.

For the analysis of the RWST, Fujita's approach is extended by using the dead mass mode shapes as generalized coordinates in a new modal analysis. This approach results in the following equation of motion:

$$[M]\ddot{\underline{\Psi}}(t) + [\tilde{\omega}_i^2]\underline{\Psi}(t) = -\underline{F}\ddot{z}(t) \qquad (4.10a)$$

where:

$$M_{ij} = \int_0^H m(x)\,\tilde{\phi}_i(x)\tilde{\phi}_j(x)dx$$

$$+\rho\pi R\sum_{k=0}^{\infty}\left(\frac{2I_1(\lambda_k R)}{\lambda_k I_i'(\lambda_k R)}\int_0^H \tilde{\phi}_i(x)\cos(\lambda_k x)dx\int_0^H \tilde{\phi}_j(\xi)\cos(\lambda_k\xi)d\xi\right) \qquad (4.10b)$$

$$F_i = \int_0^H m(x)\tilde{\phi}_i(x)dx + \rho\pi R\sum_{j=0}^{\infty}\left(\frac{2I_1(\lambda_j R)}{\lambda_j I_i'(\lambda_j R)}\int_0^H \cos(\lambda_j\xi)d\xi\int_0^H \phi_i(x)\cos(\lambda_j x)dx\right) \qquad (4.10c)$$

Note that the generalized coordinates are coupled only through the off-diagonal of the mass matrix. As the fluid in the tank has no stiffness, the stiffness matrix remains diagonal. Equation (4.10) is solved using standard modal analysis/response spectrum analysis methods. The displacement of the tank wall and the pressure distribution on the tank wall are then found by transforming back through the empty tank generalized coordinates:

$$w(x,t) = \sum_{i=1}^{N}\tilde{\phi}_i(x)\Psi_i(t) \qquad (4.11a)$$

$$p(x,t) = \sum_{i=1}^{N} p_i(x)\Psi_i(t) \qquad (4.11b)$$

The above beam analysis method assumes that the dead mass normal modes of the tank form an adequate basis for the normal modes of the fluid/tank system. To establish the validity of that assumption, the fundamental mode's frequency, participation factor, base moment, and base shear calculated using this beam analysis method are compared, in Figure 5, to Haroun's results. Haroun's results, which are based on a shell finite element discretization of the tank wall and a boundary element discretization of the fluid, can be considered "exact."

Figure 5 shows that the beam analysis deviates significantly from the shell analysis for low values of H/R. As H/R increases, the difference between the two analyses decreases. For H/R = 3.4, the maximum value considered by Haroun, the modal properties differ by less than 5%. From these results it is concluded that for the RWST -- which has an H/R ratio of 6.1 -- the beam model and the shell model would yield essentially identical results.

The beam analysis method was applied to the RWST using the model shown in Figure 6. The tank shell is discretized using ten beam elements. Both bending and shear deformation are considered. A rotational spring at the base is used to model the anchor bolts' flexibility. The spring value is based on the assumption that the anchor bolts are free to elongate over a length of 48" (see Figure 2).

Three modes were calculated below 33 Hz. The frequencies, spectral accelerations for 7% damping, and resulting stresses in the tank wall are listed in Table 1.

In the response analysis calculation, the first two modes were analyzed individually. The tank mass and fluid pressure not participating in the first two modes was then uniformly distributed over the tank height and statically analyzed using the spectral acceleration corresponding to the third mode frequency. This "rigid-range" response and the responses from the two flexible modes and the convective mode were then combined using the SRSS method.

4.3 Vertical Seismic Response

As pointed out by Rigaudeau [18], the vertical frequency of a cylindrical tank can be calculated using the following:

$$f_v = \frac{1}{4H}\left(\frac{Eh}{2\rho R}\right)^{\frac{1}{2}} \qquad (4.12)$$

This corresponds to a mode of vibration in which the increase in pressure due to the vertical inertial forces on the fluid cause the tank walls to expand axisymmetrically. This is commonly referred to as the fundamental "breathing" mode of the tank. The overall mode shape is nearly identical to the deformation shape caused by the fluid hydrostatic pressure. Thus, the resultant hoop stresses can be calculated by scaling the dead load hoop stresses by the vertical spectral acceleration at the calculated frequency.

In the case of the RWST, Equation 4.12 indicates a frequency of between 4.0 Hz and 4.5 Hz (Note that Equation 4.12 assumes uniform tank wall thickness). The peak of the Ginna spectrum occurs at 5 Hz, thus the peak is used for this analysis. Using two-thirds of the horizontal spectrum and 7% damping yields a spectral acceleration of 0.265g. The resulting stresses, obtained by scaling the dead load stresses, are shown in Table 2.

4.4 Anchorage Loads

The RWST's anchorage is required to resist the overturning moment induced by horizontal seismic forces. The total overturning moment is calculated by an SRSS of the base moments of the convective mode and the three impulsive modes:

$$M_{BASE} = 2.91 \times 10^5 \text{ kip} \cdot \text{in.} \qquad (4.13)$$

The load on the anchorage due to the overturning moment is calculated by considering a cross-section of the tank shell just above the base (Figure 7). This cross section consists of a circle with the tank thickness (0.3125 in.) on the compression side and the smeared bolt thickness (0.0976 in.) on the tension side. Force equilibrium determines the

position of the neutral axis, as shown in Figure 7. Moment equilibrium establishes the relation between the base moment and the maximum bolt force (F_B):

$$F_B = 8.81 \frac{M_{BASE}}{R^2} = 101 \text{ kips} \qquad (4.14)$$

The bolt stress is calculated by dividing F_B by the tensile area of the bolt. Standard analytical techniques are used to calculate the maximum bending and shear stresses developed in the vertical bracket plates and the maximum shear stress at the critical weld point (Point A in Figure 3). The anchorage stresses are listed in Table 2. Note that the bracket is detailed so that only tensile forces are developed in the bolts. Thus the welds between the horizontal and vertical bracket plates and at the bottom of the vertical bracket plates (Points B and C in Figure 3) are not significantly stressed.

As is generally assumed in flat bottom vertical tank analysis, the base shear is considered to be resisted by friction between the tank bottom and the concrete base.

5 ACCEPTANCE CRITERIA

The acceptance criteria are based on the appropriate allowable stresses for the points listed in Tables 3 and 4. These allowable stresses are shown in Tables 3 and 4, their source is documented below:

5.1 Tank Wall Material

From Reference 1, Table I-7.2, for Type 304 stainless steel at 200°F:

$$S = 17.8 \text{ ksi} \tag{5.1a}$$

For Level D service limits, Reference 1, Table NC-3821.5-1, yields:

$$\sigma_m \leq 2S = 35.6 \text{ ksi} \tag{5.1b}$$

5.2 Anchorage Materials

5.2.1 Anchor Bolts

From Reference 1, Table I-13.1, the tensile strength of A36 steel is:

$$S_u = 58 \text{ ksi} \tag{5.2a}$$

For Level D service limits, Reference 1, paragraph F-1370, yields:

$$F_{tb} = 0.7\ S_u = 40.6 \text{ ksi} \tag{5.2b}$$

5.2.2 Bracket Material

For A-36 steel at Level D service limits, Reference 1, paragraph XVII - 2200 and F-1370 yield:

$$F_t = 1.88(0.6\ S_y) = 40.6 \text{ ksi} \quad (5.3a)$$

$$F_v = 1.88(0.40\ S_y) = 27.1 \text{ ksi} \quad (5.3b)$$

5.2.3 Weld Material

With A-36 steel as the controlling base material and Level D service limits, Reference 1, Table NF-3292.1-1 and paragraph F-1370 yield:

$$F_w = 1.88(18 \text{ ksi}) = 33.8 \text{ ksi} \quad (5.4)$$

5.3 Tank Wall Buckling

The stress state of concern in the tank wall consists of an axial compressive stress due to the moment induced by lateral seismic forces, a shear stress also induced by lateral seismic forces, and a tensile circumferential stress due to hydrostatic pressure. Evaluation of buckling for this stress state is based on tests of circular cylinders in similar states of stress.

Buckling of cylindrical shells has been the subject of extensive experimental and analytical research [3, 13, 15]. From an analysis and design perspective, the principal conclusion of that research is that theoretical buckling equations over-predict experimental results. Thus researchers have recommended knockdown factors to be applied to the theory in order to bring it into line with experimental data.

The discrepancy between theory and experimentation is attributed to imperfections in the shell geometry introduced during construction of the shell. The degree to which these imperfections -- which can be assumed to be randomly distributed through the shell -- reduce the theoretical buckling stress is a function of the uniformity of stress in the cylinder. Experimental data for three load conditions predominate in the literature: uniform axial compression, pure bending, and torsion. In the case of uniform axial compression the shell is uniformly stressed, thus buckling is controlled by the maximum imperfection in the shell. In

the case of pure bending, as the stress distribution is not uniform, it is less probable that the maximum shell imperfection coincides with the maximum compressive stress; thus the actual buckling load has been shown to be [11, 19, 22, 24] closer to the theoretical load for pure bending than for uniform axial compression. The torsional buckling stress is relatively insensitive to imperfections in the shell [3, 26].

Circumferential stresses induced by internal pressurization has also been shown to have a significant effect on the buckling of cylindrical shells [4, 6, 8-10, 22, 24-26]. In the case of buckling due to axial compression or bending, the internal pressurization reduces the level of imperfections in the tank shell, thus reducing the knockdown factor. In the case of buckling due to torsion, the circumferential stresses induced by internal pressurization interact with the shear stresses to alter the stress state in the shell. As a result, internal pressurization can increase the torsional buckling stress well above the theoretical unpressurized torsional buckling stress.

The research most relevant to the particular state of stress in the RWST is that of Harris [8] and Weingarten [26] for buckling of circular cylinders under combined axial load, torsion, and internal pressure. These stress states investigated in this research differ from that in the RWST in that the researched stress state is uniform throughout the cylinder, while the stress state in the RWST is localized. As the uniformity of the researched stress state heightens the influence of the local imperfections in the shell, the researched stress state can be considered more critical than that of the RWST.

Weingarten presents the theoretical deriviation of the following interaction equation:

$$\frac{\sigma_\phi}{\sigma_c} + \left(\frac{\tau}{\tau_c}\right)^2 = 1 \qquad (5.5a)$$

where:

$$\tau_c = \left(1 + \frac{p}{p_e}\right)^{\frac{1}{2}} \tilde{\tau}_c \qquad (5.5b)$$

and

$$P_e = 0.92E\left(\frac{R}{L}\right)\left(\frac{h}{R}\right)^{2.5} \quad (5.5c)$$

Weingarten presents confirmatory test data for the cases of internal pressure, torsion, and either no axial load or tensile axial load. Harris presents confirmatory test data for the case of internal pressure, torsion, and compressive axial load. Weingarten and Harris stipulate that the critical axial stress (σ_c) and the critical torsional stress (τ_c) should be based on empirically derived data. The critical stresses used in the RWST evaluation are discussed below.

The critical axial stress is based on the NASA design criteria [13] for cylindrical shells in pure bending:

$$\sigma_c = \frac{Eh}{R}(.605\gamma + \Delta\gamma) \quad (5.6)$$

The curves from this document defining the knockdown factor for the unpressurized case (γ), and the increase due to internal pressurization ($\Delta\gamma$), are shown in Figure 8. Note that the curves for bending rather than axial compression are used. While the theoretical critical stress is the same for both pure bending and axial compression [24], as discussed above, the effect of imperfections is less severe for pure bending than for axial compression.

The unpressurized critical shear stress is based on the NASA design criteria for cylindrical shells in pure torsion:

$$\tau_c = 0.747\gamma E\left(\frac{R}{L}\right)^{0.5}\left(\frac{h}{R}\right)^{1.25} \quad (5.7)$$

NASA suggests a knockdown factor (γ) of 0.67. This knockdown factor is however based on tests of cylinders in pure torsion. Lundquist [12] performed tests on cylinders loaded in transverse shear. These tests

showed an increase in the critical shear stress of a factor of at least 1.25 over the critical shear stress for a pure torsional load. Thus, as the RWST is loaded in transverse shear, a knockdown factor of 0.84 is used in Equation (5.7). The effect of internal pressurization on the critical shear stress (Equation (5.5b)) has been confirmed by a number of other researchers [4, 8, 10].

Some research has been done on the buckling of cylindrical shells internally pressurized by a water head and subjected to a horizontal base excitation. Scale model tests by Shih and Babcock [20, 21] indicate that due to the combined effect of the water pressure and the localized nature of the maximum stress, the actual buckling stress is much closer to the theoretical value than is normally assumed in tank design. Full scale tank tests by Niwa and Clough [14] showed similar results. Specifically, shaking table tests of a stainless steel tank 9.5' in diameter, 20' in height, and 0.078" thick, yielded a critical axial stress of 14.8 ksi. The criteria presented in this report yields a critical stress of 14.3 ksi.

The results of the buckling evaluation of the RWST are summarized in Table 4. Safety factors for bending alone, shear alone, and combined bending and shear are presented for each of the three elevations of interest. Note that for the worst case of combined bending and shear to exist, the maximum response of the RWST to both horizontal earthquakes must occur simultaneously -- a very conservative assumption. Thus, a factor of safety between those shown in Table 4 for bending alone and combined bending and shear is a more appropriate indicator of the available margin against buckling.

The factors of safety presented in Table 4 are the margin with respect to the critical buckling stress. The critical buckling stress is not associated with general instability or overall collapse, but rather the onset of localized shell buckling, typically at the shell base. It is well established, most recently by full-scale testing by Niwa and Clough [14], that vertical ground supported tanks of the aspect ratio of the RWST exhibit real and significant post-buckling strength.

As discussed in Reference 27, the standard design factor of safety presented in Appendix F of the ASME Code for buckling of shell-type nuclear components at the Service Level D design condition is 1.33. For the design of component supports at the same Service Level D design condition, the factor of safety presented in Appendix F is increased to 1.5. Comparing this safety factor of 1.5 to the values shown in Table 4, it can be seen that for Service Level D conditions, the tank meets the more conservative component support requirements of Appendix F.

6. SUMMARY

The results of this evaluation are summarized in Table 3 and Table 4.

Table 3 presents the safety factors against the exceedance of material allowable stresses calculated per Reference 1. All material stress requirements are met.

Table 4 presents the safety factors against buckling of the tank wall calculated as specified in Section 5.3. Per the discussion in Section 5.3, these safety factors indicate sufficient margin against buckling of the tank wall during a seismic event.

7. SYMBOLS

d_s	=	maximum slosh height
E	=	Young's modulus of the tank material
EI	=	bending stiffness of the tank cross-section
f_s	=	frequency of the fundamental convective mode
f_v	=	frequency of the fundamental vertical mode
$\underline{F}$	=	inertial force vector of the fluid/structure system (beam analysis method)
F_B	=	maximum tensile bolt force developed due to the overturning moment
F_t	=	allowable tensile stress in the bolt bracket
F_{tb}	=	allowable tensile stress in the bolt
F_v	=	allowable shear stress in the bolt bracket
F_w	=	allowable weld stress
g	=	acceleration of gravity
GA_s	=	shear stiffness of the tank cross-section
h	=	tank wall thickness
H	=	total height of water in the tank
H_s	=	effective height of the fundamental convective mode
I_1	=	modified Bessel function of the first order
I_1'	=	first deriative of I_1
L	=	height of the tank cylinder
m	=	tank wall mass per unit length
$[M]$	=	mass matrix of the fluid/structure system (beam analysis method)
M_{BASE}	=	maximum overturning moment
N	=	number of dead mass modes used as generalized coordinates in the beam analysis method
p	=	force per unit length on the tank wall due to the impulsive fluid pressure
p_i	=	i^{th} mode's force per unit length on the tank wall due to the impulsive fluid pressure (Fujita's approach)
P	=	internal pressure in the tank due to the water's dead weight
P_e	=	external pressure at which the tank wall buckles
R	=	tank radius
S	=	allowable stress per Reference 1, Table I-7.0
S_u	=	tensile strength per Reference 1, Table I-2.0
S_y	=	yield strength per Reference 1, Table I-13.0
t	=	time
w	=	lateral displacement of the tank wall relative to the tank base
x	=	tank elevation (x=o at the tank base)
z	=	absolute displacement of the tank base

Γ_i = i^{th} mode's participation factor (Fujita's approach)

$\hat{\psi}_i$ = i^{th} dead mass mode shape

ψ_i = i^{th} generalized coordinate response (beam analysis method)

λ_i = $(i + 1/2)\pi/H$

ν = Poisson's ratio

ρ = mass density of water

σ_c = axial stress due to bending at which the tank wall buckles (including the effect of internal pressure)

σ_m = maximum membrane stress in the tank wall

σ_θ = circumferential membrane stress in the tank wall

σ_ϕ = axial membrane stress in the tank wall

τ = shear stress in the tank wall

τ_c = shear stress at which the tank wall buckles (including the effect of internal pressure)

$\hat{\tau}_c$ = shear stress at which the tank wall buckles (excluding the effect of internal pressure)

ω_i = i^{th} fluid/structure frequency (Fujita's approach)

$\hat{\omega}_i$ = i^{th} dead mass frequency

8. REFERENCES

1. ASME, Boiler and Pressure Vessel Code, Section III, Division I, 1980.

2. ASME, Cases of ASME Boiler and Pressure Vessel Code, Case N-284.

3. Baker, E. H., Kovalevsky, L., Rish, F. L., Structural Analysis of Shells, R. E. Krieger Publishing Company, Huntington, New York, 1981.

4. Crate, H., Batdorf, S. B. and Baab, G. W., "The Effect of Internal Pressure on the Buckling Stress of Thin-Walled Circular Cylinders Under Torsion," NACA L4E27, May 1944.

5. Fujita, K., and Shiraki, K., "Approximate Seismic Response Analysis of Self-Supported Thin Cylindrical Liquid Storage Tanks," Transactions of the 4th International Conference on Structural Mechanics in Reactor Technology, Paper K5/4, August 1977.

6. Fung, Y. C., and Sechler, E. E., "Buckling of Thin-Walled Circular Cylinders Under Axial Compression and Internal Pressure," Journal of Aeronautical Science, Vol. 24, No. 5, pp. 351-356, May 1957.

7. Haroun, M. A., "Vibration Studies and Tests of Liquid Storage Tanks," Earthquake Engineering and Structural Dynamics, Vol. II, pp. 179-206, 1983.

8. Harris, L. A., Suer, H. S., and Skene, W. T., "The Effect of Internal Pressure on the Buckling Stress of Thin-Walled Circular Cylinders Under Combined Axial Compression and Torsion," Journal of the Aeronautical Sciences, Vol. 25, No. 2, pp. 142-143, February 1958.

9. Harris, L. A., Suer, H. S., and Skene, W. T, "The Stability of Thin-Walled Unstiffened Circular Cylinders Under Axial Compression Including the Effects of Internal Pressure," Journal of Aeronautical Science, Vol. 24, No. 8, pp. 587-596, August 1957.

10. Hopkins, H. G., and Brown, E. H., "The Effect of Internal Pressure on the Initial Buckling of Thin-Walled Circular Cylinders Under Torsion," Aeronautical Research Council R&M, No. 2423, January 1946.

11. Lundquist, E. E., "Strength Tests of Thin-Walled Duralumin Cylinders in Pure Bending," NACA TN479, December 1933.

12. Lundquist, E. E., "Strength Tests of Thin-Walled Duralumin Cylinders in Combined Transverse Shear and Bending," NACA TN523, 1935.

13. NASA, NASA Space Vehicle Design Criteria -- Buckling of Thin-Walled Cylindrical Shells, NASA SP-8007, August 1968.

14. Niwa, A., and Clough, R. W., "Buckling of Cylindrical Liquid-Storage Tanks Under Earthquake Loading," Earthquake Engineering and Structural Dynamics, Vol. 10, pp. 107-122, 1982.

15. NUREG/CR-0793, Buckling Criteria and Application of Criteria to Design of Steel Containment Shells, March 1979.

16. NUREG/CR-1161, Recommended Revisions to Nuclear Regulatory Commission Seismic Design Criteria, May 1980, pp. 28-30, 114-120.

17. NUREG/CR-1821, Seismic Review of the Robert E. Ginna Nuclear Power Plant as Part of the Systematic Evaluation Program, November 1980, p. 85.

18. Rigaudeau, J., "Modal and Response Spectrum Analysis of Thin Cylindrical Liquid Storage Tanks," Transactions of the 6th International Conference on Structural Mechanics in Reactor Technology, Paper K8/8, August 1981.

19. Seide, P., and Weingarten, V. I., "On the Buckling of Circular Cylindrical Shells Under Pure Bending," ASME Journal of Applied Mechanics, pp. 112-116, March 1961.

20. Shih, C. F., and Babcock, C. D., "Buckling of Cylindrical Tanks Under Earthquake Excitation," Proceedings of the Third ASCE Engineering Mechanics Division Specialty Conference, September 1979.

21. Shih, C. F., and Babcock, C. D., "Scale Model Buckling Tests of a Fluid Filled Tank Under Harmonic Excitation," ASME Pressure Vessel and Piping Conference, August 1980.

22. Suer, H. S., Harris, L. A., Skene, W. T., and Benjamin, R. J., "The Bending Stability of Thin-Walled Unstiffened Circular Cylinders Including the Effects of Internal Pressure," Journal of the Aeronautical Sciences, Vol. 25, No. 5, May 1958.

23. USNRC Letter LS05-81-06-068, "Site Specific Ground Response Spectra for SEP Plants Located in the Eastern United States," June 17, 1981.

24. Weingarten, V. I., "Effects of Internal Pressure on the Buckling of Circular Cylindrical Shells Under Bending," Journal of the Aerospace Sciences, pp. 804-807, July 1962.

25. Weingarten, V. I., Morgan, E. J., and Seide, P., "Elastic Stability of Thin-Walled Cylindrical and Conical Shells Under Combined Internal Pressure and Axial Compression," AIAA Journal, Vol. 3, No. 6. June 1965.

26. Weingarten, V. I., "The Effect of Internal Pressure and Axial Tension on the Buckling of Cylindrical Shells Under Torsion," Proceedings of the Fourth U. S. National Congress of Applied Mechanics, June 1962.

27. Bohm, G.J. and Stevenson, J.D., "Extreme Loads and Their Evaluation with ASME Boiler and Pressure Vessel Code Limits, Section 5.9," Pressure Vessels and Piping Design Technology - 1982, American Society of Mechanical Engineers.

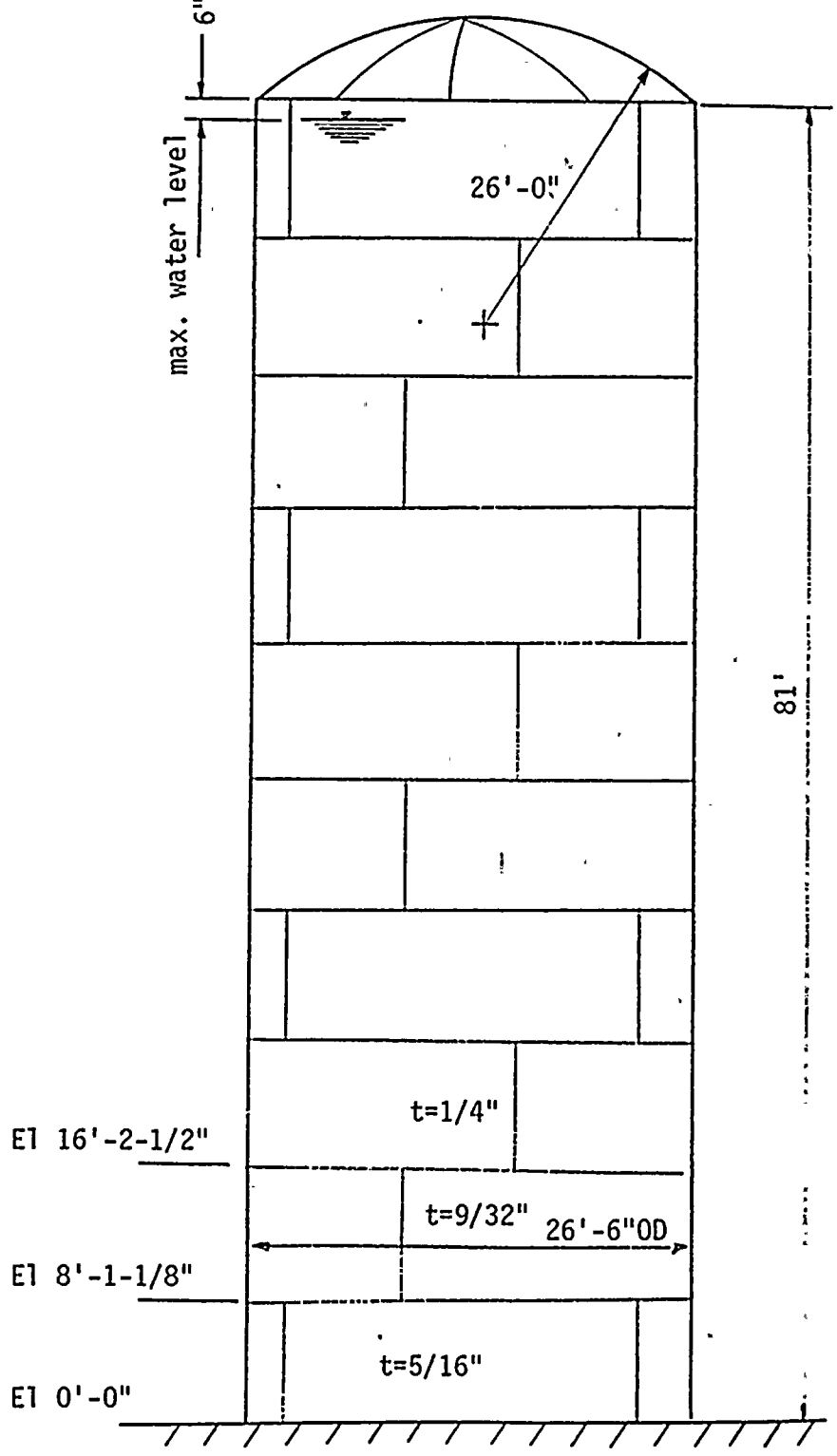

FIGURE 1
RWST ELEVATION

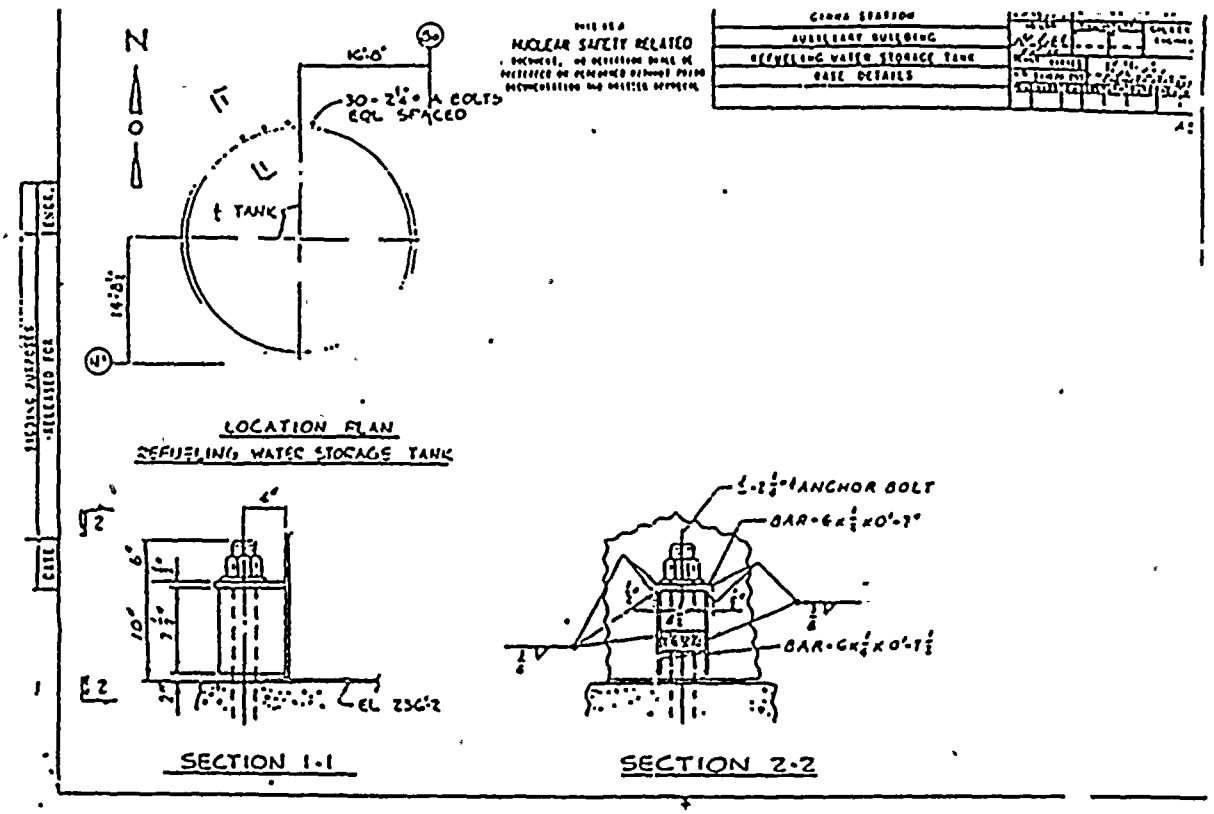

VESTINGHOUSE ELECTRIC CORPORATION
ATOMIC POWER DIVISION
R.G.&E. CORP., ROCHESTER, N.Y.

GILBERT ASSOCIATES, INC.
ENGINEERS AND CONSULTANTS

STANDARD TYPES | SPECIAL TYPES

NOTES:-

FIGURE 2

RWST BASE ANCHORAGE DETAILS

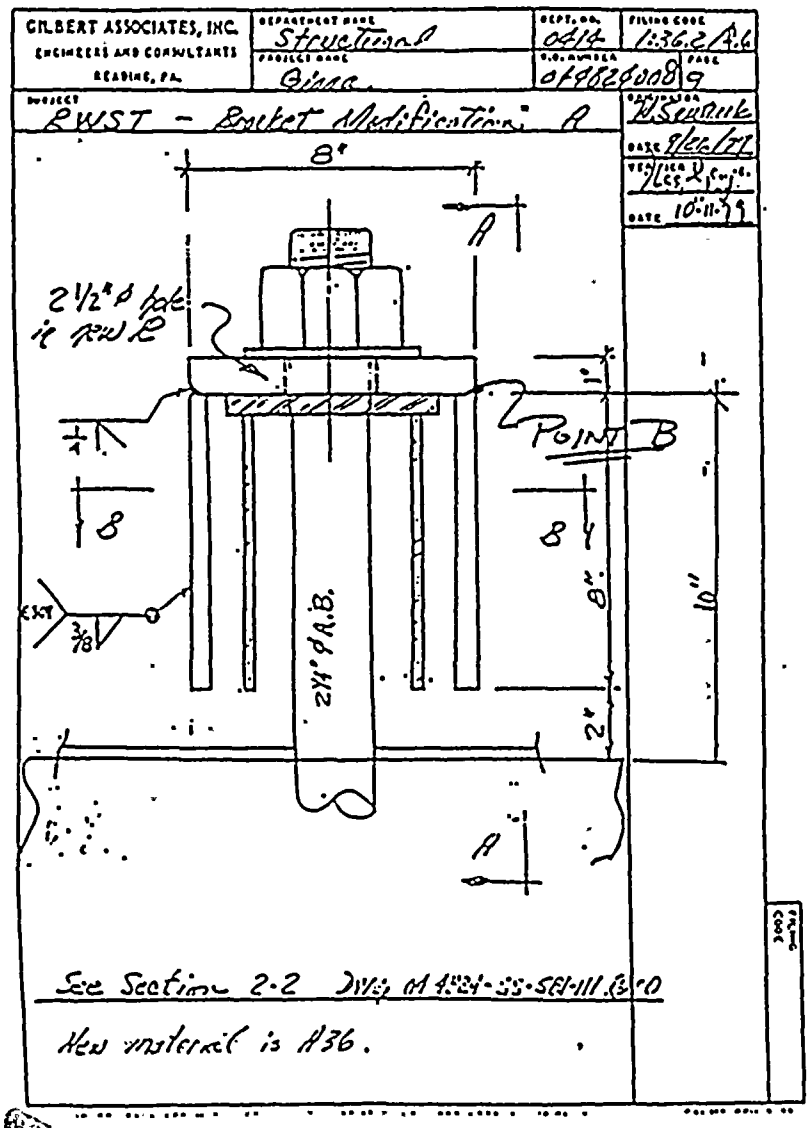

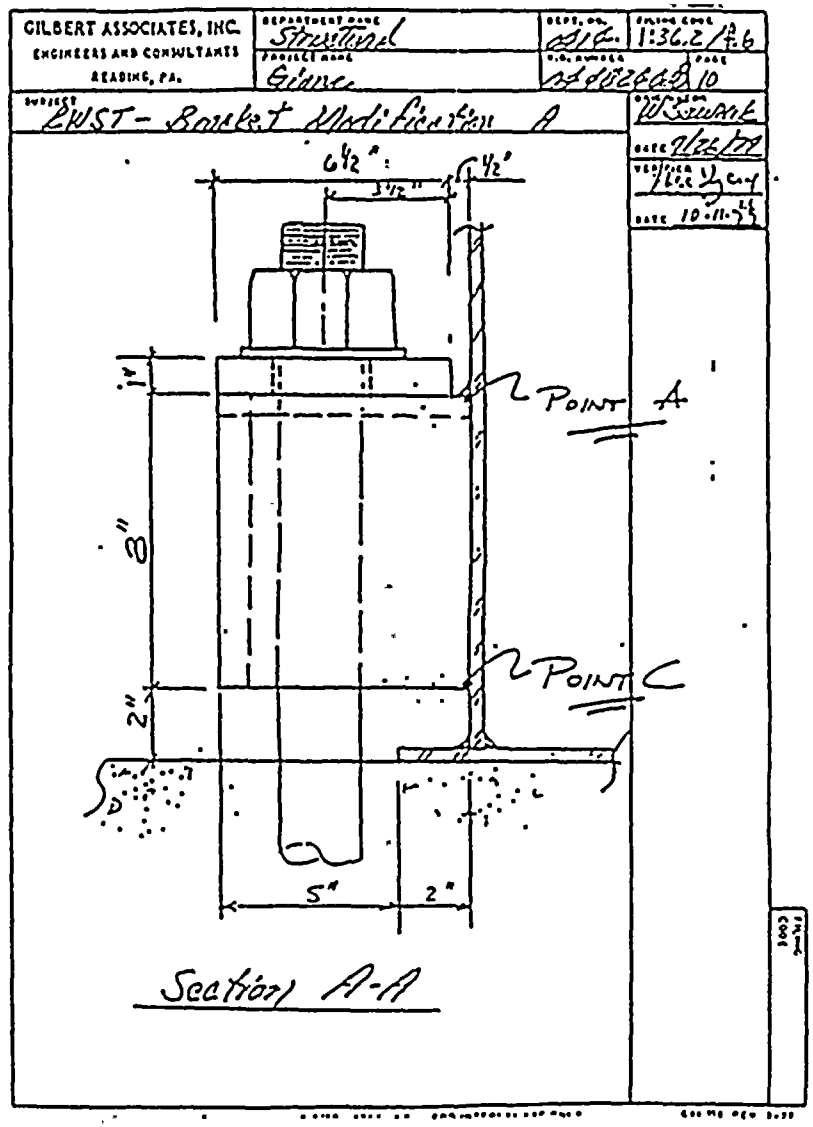

FIGURE 3
RWST BASE ANCHORAGE DETAILS

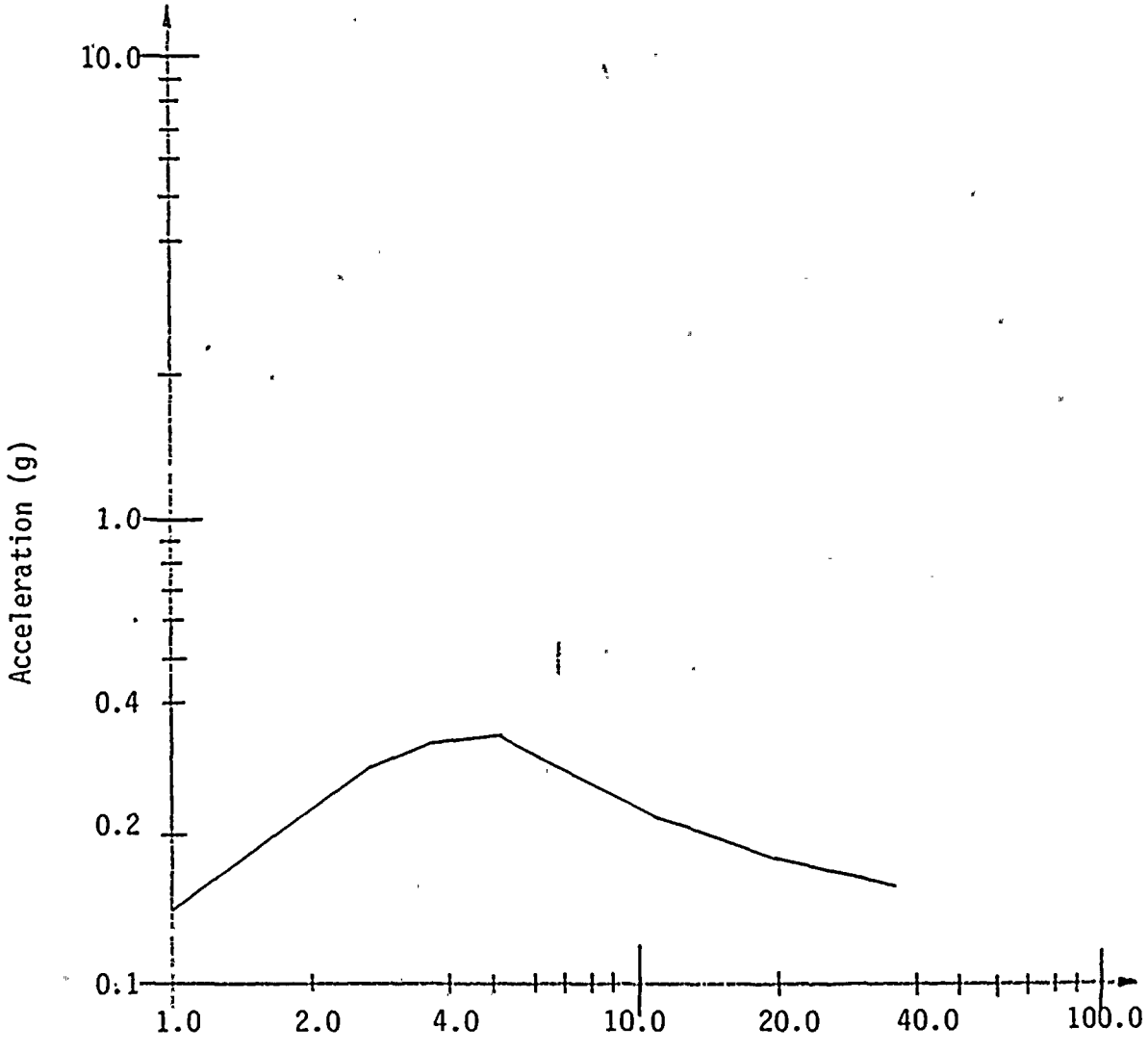

FIGURE 4
USNRC SITE SPECIFIC GROUND RESPONSE
SPECTRUM FOR R. E. GINNA (7% DAMPING)

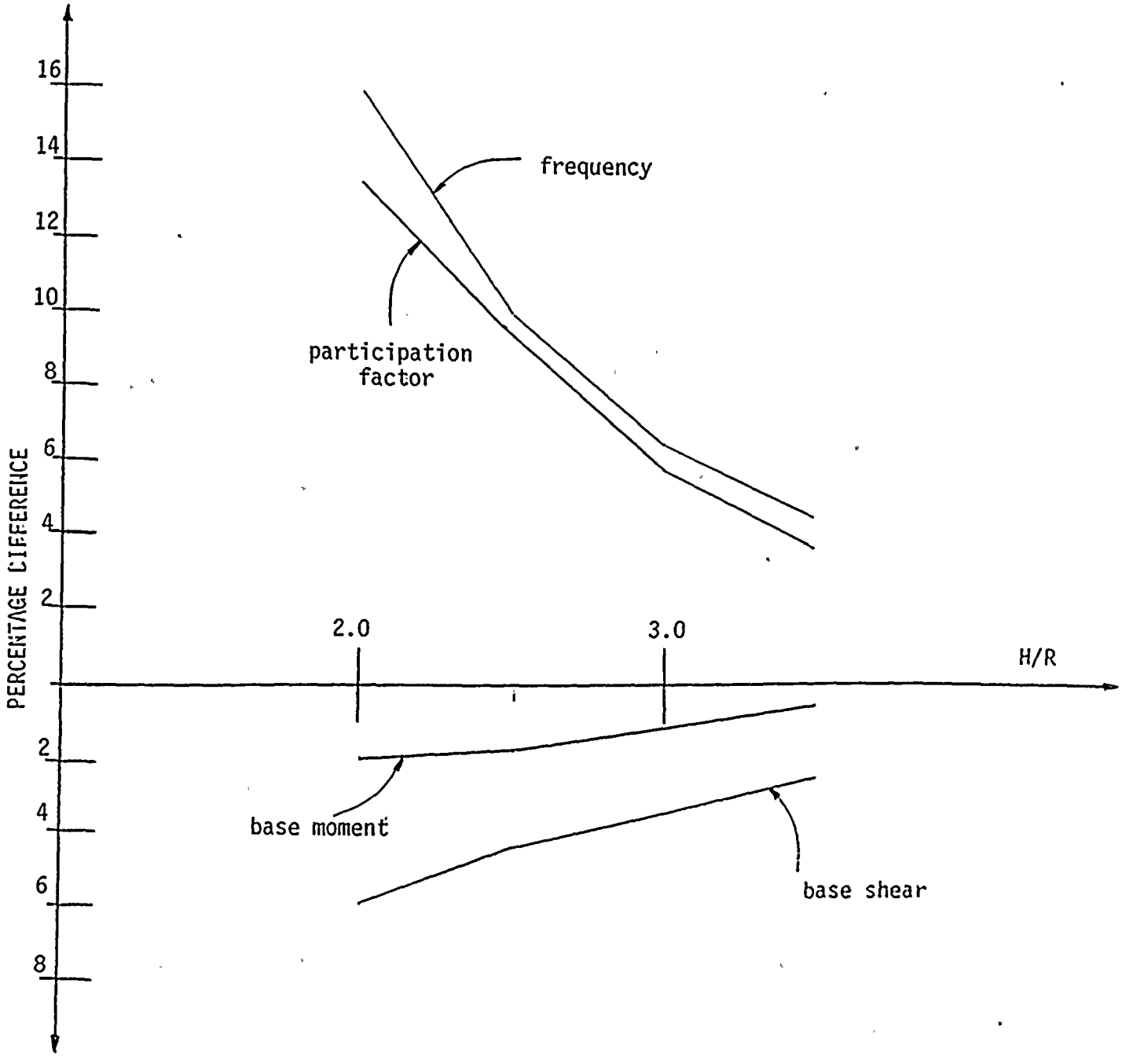

FIGURE 5

PERCENTAGE DIFFERENCE IN THE FUNDAMENTAL MODE PARAMETERS BETWEEN HAROUN'S SHELL ANALYSIS (REFERENCE 7) AND THE BEAM ANALYSIS USED FOR THE RWST

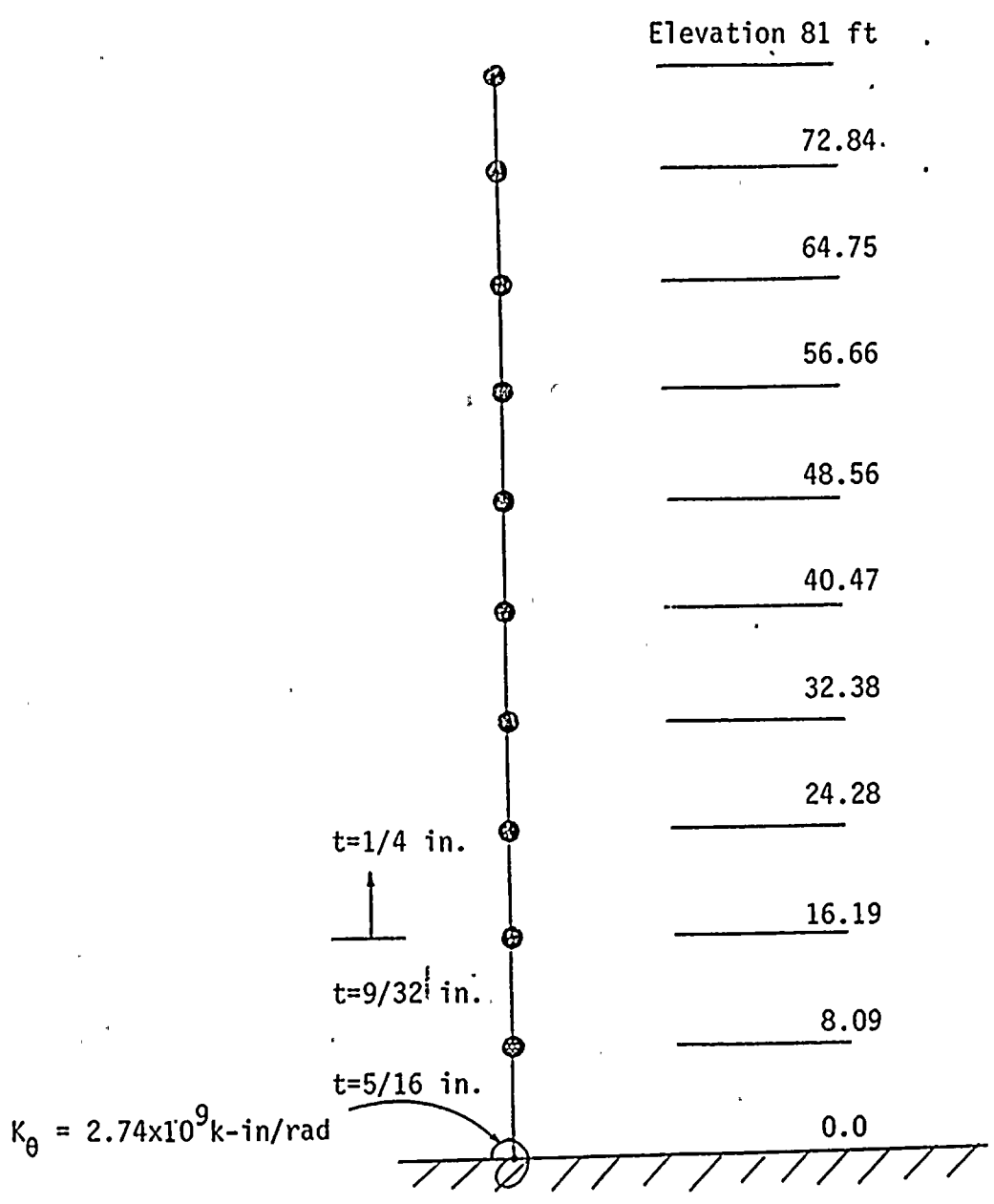

FIGURE 6

RWST BEAM MODEL

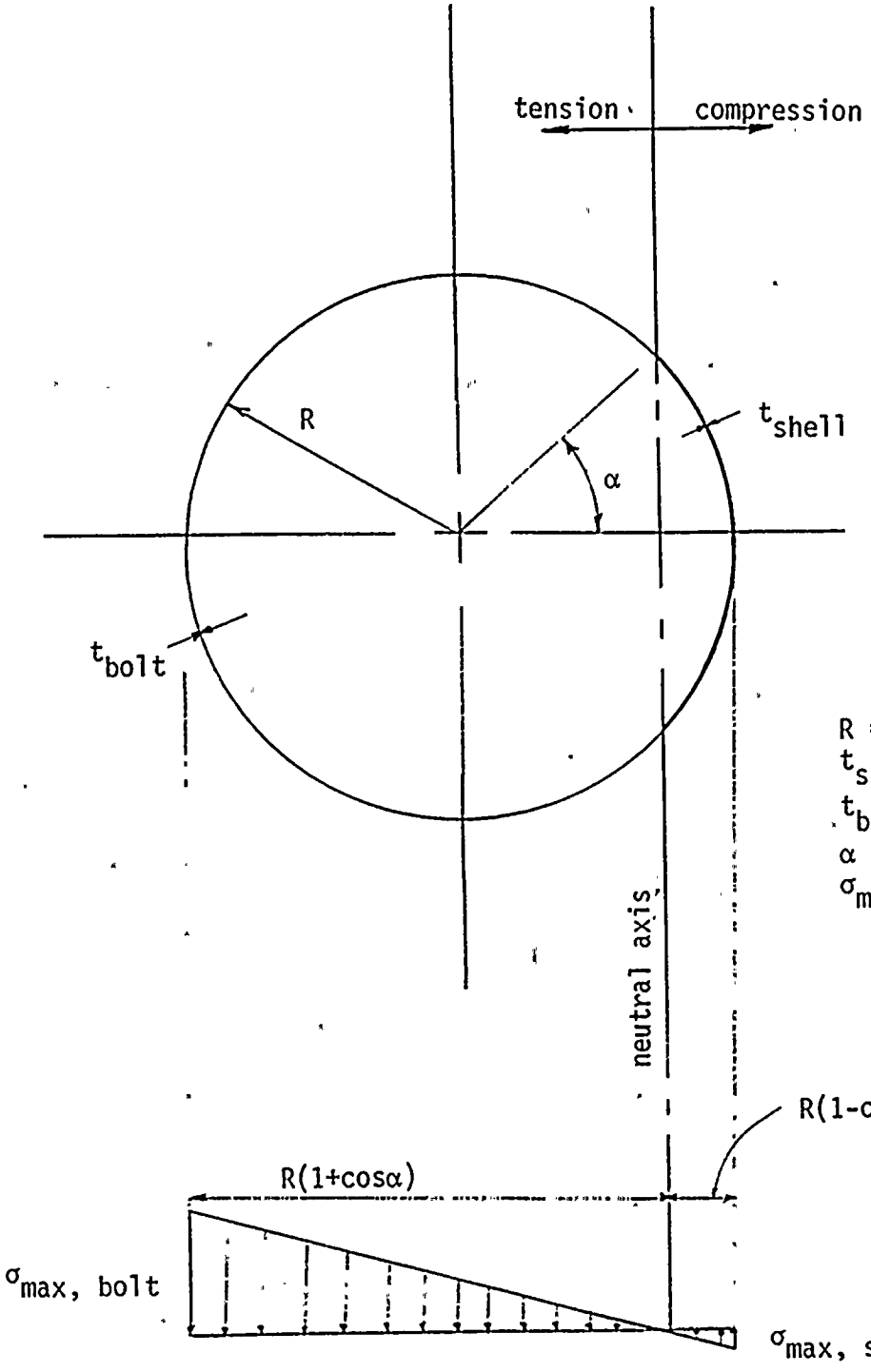

R = 159 in.
t_{shell} = 0.3125 in.
t_{bolt} = 0.098 in.
α = 70°
$\sigma_{max, shell} = \frac{1-\cos\alpha}{1+\cos\alpha} \sigma_{max, bolt}$

FIGURE 7

STRESS DISTRIBUTION AT THE BASE OF RWST
DUE TO OVERTURNING MOMENT

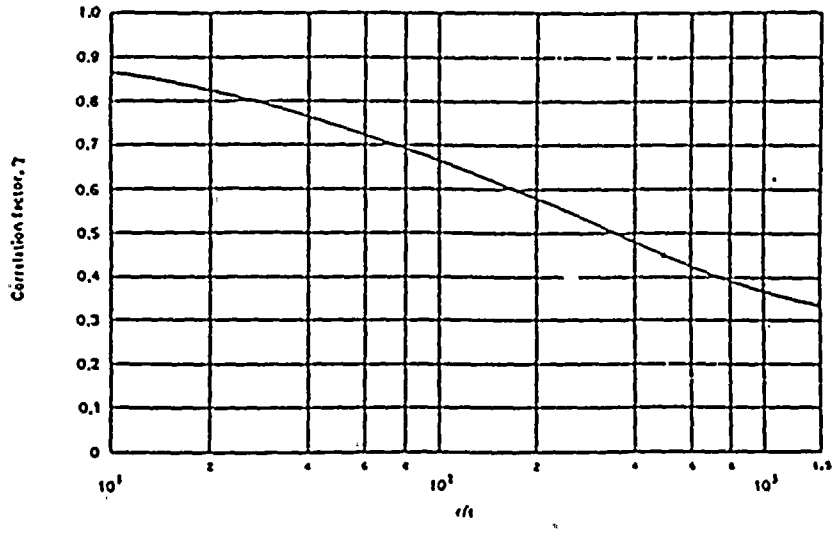

Figure 3
Correlation factors for isotropic circular cylinders subjected to bending

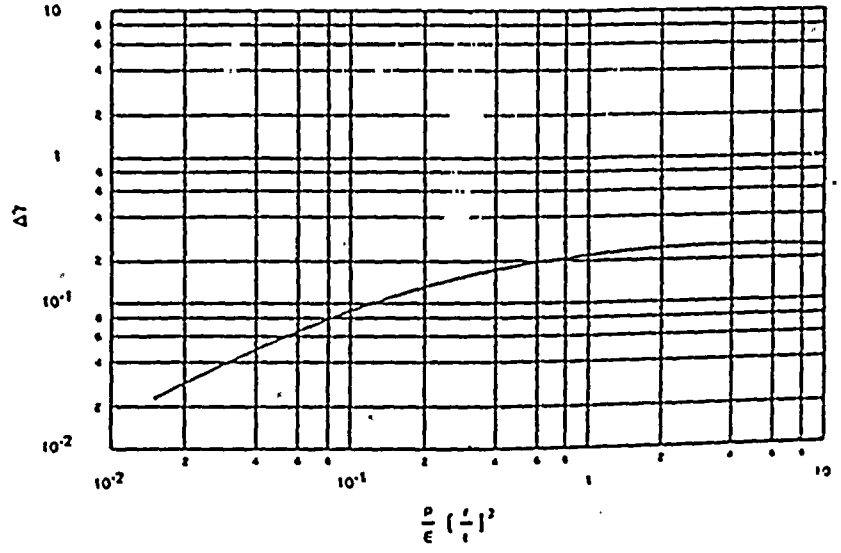

Figure 6
Increase in axial-compressive buckling-stress coefficient of cylinders due to internal pressure.

FIGURE 8
BUCKLING CURVES FROM REFERENCE 13
FOR USE IN EQUATION 5.6

	CONVECTIVE MODE	IMPULSIVE MODES		
		MODE 1	MODE 2	MODE 3*
Frequency (Hz)	0.34	2.00	8.55	19.2
Spectral Acceleration (g)	.097	.260	.276	.200
El. 16'-2-1/4"				
Maximum Bending Stress (ksi)	0.7	10.1	0.4	0.7
Maximum Shear Stress (ksi)	0.2	3.6	0.9	0.4
El. 8'-1/8"				
Maximum Bending Stress (ksi)	0.7	10.9	0.2	0.9
Maximum Shear Stress (ksi)	0.1	3.3	1.0	0.4
El. 0'-0"				
Maximum Bending Stress (ksi)	0.7	11.7	0.7	1.1
Maximum Shear Stress (ksi)	0.1	3.0	1.0	0.4

*Rigid range effects are included

TABLE 1 SUMMARY OF THE HORIZONTAL MODAL RESPONSES

	DEAD LOAD	HORIZONTAL SEISMIC	VERTICAL SEISMIC	TOTAL
TANK WALL				
El. 16'-2-1/4"				
Hoop Stress	17.7	0.6	4.7	22.4
Axial Stress	0.3	10.1	0.1	10.4
Shear Stress	--	3.7	--	3.7
El. 8'-8-1/8"				
Hoop Stress	17.7	0.6	4.7	22.4
Axial Stress	0.3	11.0	0.1	11.3
Shear Stress	--	3.4	--	3.4
El. 0'-0"				
Hoop Stress	17.7	0.5	4.7	22.4
Axial Stress	0.2	11.7	0.1	11.9
Shear Stress	--	3.2	--	3.2
ANCHORAGE				
Bolt Stress	--	31.2	--	31.2
Bracket				
Tensile Stress	--	14.0	--	14.0
Shear Stress	--	8.4	--	8.4
Weld Stress	--	22.7	--	22.7

TABLE 2 STRESS SUMMARY (ALL UNITS ARE KSI)

	MAXIMUM STRESS (KSI)	ALLOWABLE STRESS (KSI)	FACTOR OF SAFETY
TANK WALL			
El. 16'-2-1/4"	22.8	35.6	1.56
El. 8'-1/8"	22.7	35.6	1.57
El. 0'-0"	22.7	35.6	1.57
ANCHORAGE			
Bolt Stress	31.2	40.6	1.30
Bracket			
Tensile Stress	14.0	40.6	2.90
Shear Stress	8.4	27.1	3.23
Weld Stress	22.7	33.8	1.49

TABLE 3 FACTORS OF SAFETY AGAINST MATERIAL OVERSTRESS

	MAXIMUM STRESS (KSI)	ALLOWABLE STRESS (KSI)	FACTOR OF SAFETY
TANK WALL			
El. 16'-2-1/4"			
Bending	10.4	19.2	1.85
Shear	3.7	18.4	4.97
Combined	--	--	1.72
El. 8'-1-1/8"			
Bending	11.3	21.0	1.86
Shear	3.4	19.6	5.76
Combined	--	--	1.76
El. 0'-0"			
Bending	11.9	23.4	1.97
Shear	3.2	20.8	6.50
Combined	--	--	1.88

TABLE 4 FACTORS OF SAFETY AGAINST BUCKLING